The Thesis Committee for Yu Yang Xie
Certifies that this is the approved version of the following thesis:

A Model Based Approach for Evaluating Human Neuromusculoskeletal System Performance

APPROVED BY
SUPERVISING COMMITTEE:

Supervisor:

Dragan Djurdjanovic

Jonathan Dingwell

A Model Based Approach for Evaluating Human Neuromusculoskeletal System Performance

by

Yu Yang Xie, B.E

Thesis

Presented to the Faculty of the Graduate School of

The University of Texas at Austin

in Partial Fulfillment

of the Requirements

for the Degree of

MASTER OF SCIENCE IN ENGINEERING

The University of Texas at Austin

May 2016

Acknowledgements

Foremost, I would like to express my sincere gratitude to my advisor Dr.Dragan Djurdjanovic for his continuous support and valuable guidance in my master study and research. Without him, it is not possible for me to go into the area of prognostics and health monitoring, not to say getting a job in the related field. I would also like to thank Dr.Jonathan Dingwell for his review of this thesis.

I would like to thank my colleagues in LIMES lab: Deyi Zhang, Keren Wang, Asad UI Haq, Zicheng Cai and Te Ken, for their never-ending encouragements and insightful comments.

My sincere thanks also goes to Alex Bleakie and Dhruv Gupta for providing me the first data set, and to John Radke and Dr.Dragan Djurdjanovic for providing me the second data set.

Finally, I wish to thank my parents Shujuan Ye and Wenyong Xie for their love and company throughout my life, and my dear friend Shiyao Cai, for her persistent encouragement in my master study.

Abstract

A Model Based Approach for Evaluating Human Neuromusculoskeletal System Performance

Yu Yang Xie, M.S.E

The University of Texas at Austin, 2016

Supervisor: Dragan Djurdjanovic

In the thesis, a model based approach is proposed for monitoring the performance of a human neuromusculoskeletal (NMS) system. It utilizes a linear dynamic model with exogenous inputs (ARMAX model) to link multiple features extracted from surface electromyographic (sEMG) signals as model inputs, and measurable physiological outputs, such as forces produced by the limbs or limb velocities, as model outputs. This multiple-input and multiple-output (MIMO) model is then utilized to quantify and track changes in the NMS system dynamics over time. The changes in NMS system dynamics were modeled using distance between the distribution of 1-step ahead model prediction errors observed at the beginning of the exercise, when the subject was rested, and 1-step ahead prediction errors observed at any other time during exercise. The distance, referred to as the Freshness Similarity Index (FSI), was expressed via the Kullback Leibler (KL) divergence measure between the aforementioned distributions of 1-step ahead prediction errors. As the subjects proceeded with their exercises and got increasingly tired, the modeling errors were expected to increase, leading to an increase in FSI. Such behavior of FSIs enables it to act as a quantitative measure of the level of changes in NMS system performance, in other words, as a measure of NMS system performance degradation due to fatigues. The methodology has been evaluated on two data sets, one collected from an activity related to

lower limb muscles and the other collected from temporomandibular joint (TMJ) muscles. In both cases, an increasing trend in the FSI clearly illustrated changes in NMS system performance, as exercise progressed. Furthermore, after rest, FSI observed in both exercises recovered to their original levels, quantitatively and meaningfully showing that the corresponding NMS systems of the two subjects indeed rested.

Table of Contents

List of Figures

List of Tables

Chapter 1.
Introduction

Condition-based monitoring of machines has been an indispensable component to many engineering systems for preventing machine downtime and optimizing system operations [1]. Human bodies can be seen as exceptionally complicated machines and there could be great benefits in applying the well-developed methodologies from machine monitoring to facilitate continuous quantitative monitoring of the performance and health of human body systems. Furthermore, recent development and proliferation of wearable non-intrusive biosensor systems, wireless communication and powerful pervasive computing platforms are enabling even further the vision of continuous on-line monitoring of human bodies, using similar concepts to what we see today in machine monitoring and maintenance.

Typically, machine monitoring employs one of the two philosophies: symptom-based methods or model-based methods [2]. Symptom-based methods focus on detecting variations in the collected signals to identify performance changes of the corresponding systems, with abnormal signal patterns being associated with abnormal system behaviors. An implicit assumption underlying this concept is stationarity of system inputs, which then leads to consistency of system behavior and changes when degradation occurs. Nevertheless, this is not true for virtually all biomedical systems and hence, the use of symptom-based methods is greatly limited for applications in monitoring of human body systems.

Model-based methods for monitoring of system performance and condition are alternatives that rely on the use of both inputs and outputs of the underlying systems. With this paradigm, we need to build dynamic models between system inputs and outputs, and the system performance changes are tracked by quantitatively capturing changes in the model, or in other words, changes in system dynamics. By exploiting the dynamic relationships between system inputs and outputs,

model-based methods can robustly monitor system performance even when the inputs are non-stationary. Such a monitoring paradigm is capable of distinguishing between system behavior changes caused by actual changes in system dynamics, and the changes caused by changes in input regimes. In addition, tracking the model rather than relevant signals provides information about what portions of system dynamics (what model parameters) are responsible for changes of system behavior, which could be of tremendous diagnostic value (important for identifying the root causes why the system degradation is occurring). Therefore, model-based methods have overwhelming advantages for monitoring human body systems and systems in general, when compared to symptom based methods [3].

While model-based diagnostics remains impractical or even impossible for many biomedical systems, the neuromusculoskeletal (NMS) system is ripe for this diagnostic paradigm shift because its inputs and outputs are more or less measurable using available sensing technologies, and significant work has already been done to relate the two. Namely, limb force and movement arise from muscle contractions, which are induced via electrical signals from the central and peripheral nervous system. Effects of these electrical stimulations of the muscles are indirectly measurable through surface electromyography (sEMG) electrodes, which can therefore be seen as inputs into the NMS system. Furthermore, kinematics and motion variables in terms of limb output force and velocities constitute the outputs from the NMS system and are also measurable via dynamometers, accelerometers or vision based motion capture systems. A model-based monitoring scheme for the NMS system could continuously track and characterize changes in the NMS system dynamics without the need to necessarily prescribe motion patterns that a subject needs to perform. Such capability could facilitate personalizing and customizing of training regimens for athletes and patients undergoing rehabilitation by prescribing exercises that target the muscles and joints with the greatest deficits for a given person, at a given time, as assessed via the system model. Furthermore, therapeutic exercise regimens for patients with NMS impairments can thus be more

precisely tailored toward returning the patient to a nominally healthy set of joint dynamics. In addition, such input-output dynamics based approaches to detection and characterization of NMS changes could more reliably indicate when to stop training or rehabilitation before the onset of injury.

When it comes to performance condition monitoring of various portions of the NMS system, prior research was almost exclusively symptom based, focused on tracking changes in either EMG signatures [4], or kinematic trajectories [5], or limb forces [6], independently. A notable exception is a recent publication [7], where a model-based method for monitoring human NMS system is devised and applied to monitor NMS system performance in repetitive sawing motion. Time frequency features (instantaneous intensity and mean frequency) are extracted from sEMG signals to serve as system inputs. These features are then linked to measured joint velocities by using autoregressive model with exogenous outputs (ARX model) to describe NMS system dynamics [7]. The level of NMS system performance degradation is quantified by calculating overlaps between the distributions of 1-step ahead prediction errors corresponding to the current or most recent system behaviors, as evaluated using the model corresponding to the least degraded ("fresh") system state. This model-based monitoring approach combining both EMG signatures and joint velocities successfully tracked fatigue induced changes in the behavior of the NMS system of 12 different human subjects completing repetitive sawing motions until voluntary exhaustion.

Despite the aforementioned advancements in model-based monitoring of NMS system, there are several issues the previous research has not addressed. Firstly, though the system degradation was clearly visible in the changes in model coefficients and modeling errors in [7], recovery of the system due to rest was not analyzed using the model-based monitoring paradigm. Furthermore, the approach is only applied to a specific repeatable cyclic motion, while the feasibility to non-cyclic motions, such as static force outputs are not discussed. To deal with the aforementioned issues, in this thesis, a slightly modified model-based monitoring method from [7]

was employed for NMS system performance monitoring during fatiguing and resting stages, using sEMG signal and limb force/movement from several portions of the human NMS system.

The remainder of this thesis is structured as follows. A literature review of current research in monitoring of NMS system performance is given in Chapter 2. In Chapter 3, methods for extraction of informative signatures from relevant signals, dynamic modeling of NMS systems using those signatures and the model-based monitoring method based on those models are described. Chapter 4 details results of applying the aforementioned methods to two different data sets corresponding to two portions of the NMS system. Finally, Chapter 5 outlines the research findings of this thesis and gives potential directions for future work.

Chapter 2.
Literature Review

This chapter attempts to summarize existing health monitoring techniques and modeling methods for human NMS systems. A general introduction to biomechanics based monitoring will be covered first, followed by an overview of sEMG signature based monitoring. Finally, reviews of mathematical models for capturing NMS system dynamics are presented.

2.1. Biomechanics Based Monitoring

The characteristic of fatigue (cause of NMS system performance degradation) can be described as a difficulty of continuing the execution of physical exercises. Formally, the neuromuscular fatigue is defined as "the inability of a group of muscles to sustain the required or expected force" [8]. Therefore, the degradation processes of NMS system performances can be studied through biomechanical model, more exactly, through NMS system dynamics and kinematics. Bini et al. [9] evaluated the effect of fatigue on coordinative patterns during cycling and reported a decay of pedaling cadence during performance degradation. Chappell et al. [10] conducted experiments on stop-jump tasks for athletes and showed that both peak proximal tibial anterior shear forces and valgus moments increased when fatigue happened. Christina et al. [11] demonstrated that localized muscle fatigue of invertors and dorsiflexors would affect loading rates, peak magnitudes and ankle joint motions during running. Gates and Dingwell [12] studied how muscle fatigue affected repetitive upper extremity task performance and reported reductions in both temporal persistence of movement speed and timing errors. Although these biomechanical models were capable of quantifying NMS system performance degradation, the main purpose of these studies was to reveal relevant fatigue mechanisms in biomechanics, and therefore, the aforementioned fatigue measures are task-specific and not suitable for our purposes.

2.2. sEMG Signature Based Monitoring

Monitoring of NMS system performance degradation can also be facilitated by the use of surface electromyographic (sEMG) signals and has been well-studied for decades. sEMG signals can provide information of underneath neuromuscular activities in the muscle [13]. More exactly, during muscle activities (contraction/relaxation), the control signals from nerve system are transmitted along nerve fibers and across neuromuscular junctions, which then activate muscle fibers in the motor units (MUs) and, after complicated biomedical events, finally produce limb forces and generate motions [14]. The collected sEMG signals reveal a train of the motor unit action potentials (MUAPs), where MUAPs are the sum of a group of muscle fiber action potential (MFAP) that represents a superposition of muscle and neuron firing signals [15]. Due to these complicated ingredients, the sEMG signals are highly noisy and non-stationary that need further processing for the purpose of NMS system monitoring. In the literature, different signatures, also called features or indicators, are extracted from sEMG signals to quantitatively monitor NMS system performance degradation. Generally, these signatures can be categorized into two types: time domain signatures and frequency domain signatures, as listed in Table 1. A concise description of different types of signatures and relevant signal processing methods are given next.

2.2.1. Time Domain Signatures

Neural communication with muscle can be characterized by both amplitude modulation and frequency modulation [16]. For time domain signatures, the changes in the amplitude modulation are tracked to evaluate NMS system performance degradation due to fatigue. Gerdle et al. [17] utilized isometric fatigue experiments to verify that root mean square (RMS) of EMG magnitude was a proper measure for muscle fatigue and, it showed an increasing trend during fatigue process. Merletti et al. [17] performed an experiment on sustained isometric voluntary contractions of tibialis anterior muscles and validated that average rectified value (ARV) could be

used as a fatigue indicator. Morlock et al. [18] reported that the zero crossing rate (ZCR) of the sEMG signal could be used as a fatigue identifier during dynamic trunk flexion/extension movements, which gave properties similar to frequency domain signatures. However, ZCR were found sensitive to signal to noise ratio (SNR) and not used in the later research [19]. In general, time domain signatures are less popular in monitoring of NMS system performance during dynamic tasks.

2.2.2. Frequency Domain Signatures

Frequency domain signatures, namely median frequency (MDF) and mean frequency (MNF), are the most widely accepted signatures in monitoring of muscle fatigue during dynamic tasks. Gerdle et al. [17] collected EMG signals in maximum repeated isokinetic knee extensions and suggested MNF shifted to lower frequency during fatigue phase. Ament et al. [20] reported an decreasing trend in the MDF of the calf muscles during an exhausting treadmill exercise. As MDF and MNF have been widely validated by numerous researchers, we will not list all the papers relevant to MDF and MNF. Interested readers could find more literatures in [21]. Other than MDF and MNF, a spectral index that considered the bandwidth of sEMG signals was recently proposed by Dimitrov et al. [22]. This new spectral index was validated in dynamic knee-extension exercises and reported to have higher sensitivities to fatigue than MDF [22]. Though Dimitrov's spectral index is not as popular as MDF and MNF, it is gaining more attentions in the recent years.

When it comes to frequency domain signatures, choosing appropriate signal processing algorithms plays a vital role in the signature extraction. Typical methods include Fourier-based spectral estimators [23] and parametric based spectral estimators [24]. However, these methods did not address to the non-stationary properties of sEMG signals. As a result, the use of time frequency techniques was proposed to alleviate this issue, which enables extraction of the so-called instantaneous mean/median frequency (IMNF, IMDF) that evaluates MNF and MDF at each instant of time. These time frequency methods include short time Fourier transform (STFT) [25], Wigner

distribution (WD) [26], Cohen's class of time frequency distribution [27], wavelet methods [28], time varying autoregressive approach [29], etc. Although there are many advancements in sEMG signature based monitoring, these methods are still in the category of symptom-based monitoring and limited for the applications in monitoring of human body systems, as explained in Chapter 1.

Table 1 sEMG signatures and corresponding calculation methods

Type	Signature	Calculation Method
Time Domain	Average rectified value (ARV)	$\frac{1}{T}\sum_{t=1}^{T}\lvert s_t\rvert$
	Root mean square (RMS)	$\sqrt{\frac{1}{T}\sum_{t=1}^{T} {s_t}^2}$, where s_t is the signal
	Zero crossing rate (ZCR)	$\frac{1}{T-1}\sum_{t=2}^{T} I\{s_t s_{t-1} < 0\}$, where $I\{A\}$ is 1 if A is true and 0 otherwise
Frequency Domain	Median frequency (MDF)	$\sum_{f=0}^{MDF} P(f) = \sum_{f=MDF}^{f_s/2} P(f)$
	Mean frequency (MNF)	$\frac{\sum_{j=1}^{M} f_j P_j}{\sum_{j=1}^{M} P_j}$, where f_j the frequency value of sEMG power spectrum at j[th] index and P_j is the power spectrum at f_j
	Dimitrov's spectral index	$\frac{\int_{f_L}^{f_H} f^{-1}P(f)df}{\int_{f_L}^{f_H} f^{5}P(f)df}$, where f_L and f_H are the lowest and highest frequency of sEMG signals

2.3. Modeling of NMS Systems

To implement model-based monitoring to NMS systems, it is necessary to develop sEMG driven musculoskeletal models to describe overall NMS system dynamics. In the field of prosthetic limb control, different types of models have been developed to link sEMG signals to NMS system outputs, e.g. limb forces or velocities, for better control of prosthetic limbs. These mathematical models could roughly be categorized as physics-based models or data driven models.

Physics-based models are dynamic models derived from biological structures of relevant portions of NMS system, with model parameters calibrated for each individual. These models are generally based on Hill's muscle model [30] to evaluate muscle output forces. Manal and Buchanan [31] combines a one-parameter A-model and Hill-type model to estimate isometric joint moments

from EMG signals. Moosavi et al. [32] implemented a hybrid EMG-driven Hill-type model to predict muscle force from elbow flexors and extensors during weight training exercises with dumbbells. Lloyd and Besier [33] utilized a modified EMG driven Hill type model to evaluate muscle force and knee joint moments. However, developing physics-based models requires deep understanding to the relevant biomechanical process, which potentially limit their popularities.

Conversely, data driven models do not incorporate the use of biomechanics and learn the NMS system dynamics solely based on data (sEMG signals and physiological outputs). Arslan et al. [34] extracted higher order frequency moments from sEMG signals and trained an artificial neural network to predict externally applied forces to human hands. Zhange et al. [35] utilized polynomial Hammerstein model (PHM) to predict generated torque based on the measured sEMG signals. Artemiadis and Kyriakopoulos [36] employed an autoregressive moving average model with exogenous outputs (ARMAX model) to link sEMG signals to elbow joint angles. Since data driven models rely heavily on the collected data, the performance of data driven models will be largely affected by data quality and data selection.

To conclude, both biomechanics based monitoring methods and sEMG signature based monitoring methods have been proposed to monitoring NMS system performance, which have achieved successes in different portions of the NMS system. Biomechanics based monitoring methods are normally applied to a specific portion of NMS system and require deep understanding of biomechanics, which limits their popularity. As mentioned in Chapter 1, sEMG signature based monitoring methods fall into the category of symptom-based monitoring methods, and have their intrinsic defects in monitoring human NMS systems, when compared to the model-based monitoring methods. However, to the best of author's knowledge, only a recent publication [7] applies model-based monitoring methods to human NMS system. Therefore, this thesis attempts to extend the model-based method presented in [7] to monitor NMS system performance during exercise and recovery processes. The detailed methodologies are presented in Chapter 3.

Chapter 3.
Methodology

The proposed model-based method tracks changes in NMS system dynamics, which enables continuous monitoring of NMS system performance. The general framework is summarized in the Figure 1. The model-based monitoring starts with the processing of sEMG signals to extract informative features for building models of NMS system dynamics. It is well-established that sEMG signals are highly noisy and non-stationary, with their frequency contents significantly changing over time [13]. This brings the need for their joint time frequency analysis, rather than using more traditional purely frequency or time domain techniques [37]. In this thesis, Cohen's class of time frequency analysis [38] is used to generate joint distributions of signal energy in time and frequency domains. The time frequency distribution (TFD) $C(t,\omega)$ of a signal $s(t)$ is determined as follows.

$$C(t,\omega) = \frac{1}{4\pi^2}\iiint s^*(u-\frac{1}{2}\tau)s(u+\frac{1}{2}\tau)\phi(\theta,\tau)e^{-j(\theta(t-u)+\tau\omega)}d\tau du d\theta \quad (1)$$

where $s^*(t)$ represent the complex conjugate of $s(t)$ and $\phi(\theta,\tau)$ is the so-called time frequency kernel. Kernel characteristics can endow the resulting TFD with desirable mathematical properties and significant research on the design and selection of kernels took place in the 1980s and early 1990s, as nicely summarized in [39].

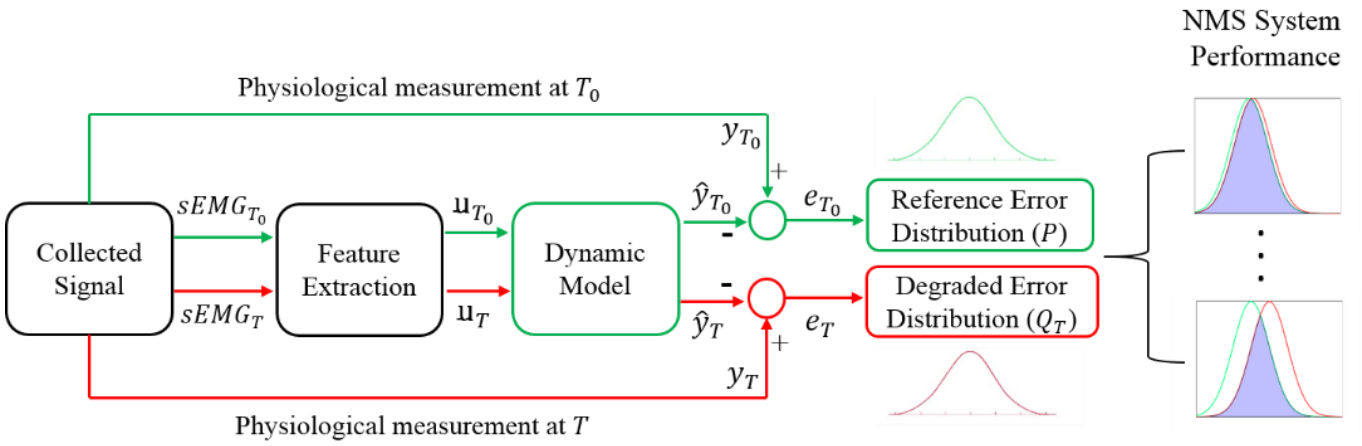

Figure 1. Model-based monitoring of NMS system

Following [7], the binomial kernel [40] is used in this thesis. It is a signal independent member of the reduced interference distribution family of kernels, which enables faster calculation of TFDs compared to signal dependent kernels, and delivers desirable mathematical properties, such as strong time and frequency support, upholding time and frequency marginal, as well as providing instantaneous frequency and group delay while reducing the interference of signals in the time-frequency plane [38]. Due to these favorable mathematical properties, the binomial kernel based TFD can be used to efficiently extract time frequency features that indicate instantaneous intensity, frequency, 2nd order moment and entropy, as listed in Table 2. Specifically, instantaneous intensity $< f^0|t >$ and instantaneous frequency $< f^1|t >$ are two features that have been widely shown to be related to muscle fatigue and performance [7,41,42]. The remaining two features, instantaneous 2nd order moment $< f^2|t >$, and instantaneous entropy $< S|t >$, are also used to provide a more accurate statistical representation of instantaneous features of the TFD. An example of a sEMG signal from human Soleus muscle performing isometric contraction and the corresponding binomial kernel TFD are presented in Figure 2, while the corresponding extracted time series of instantaneous features are shown in Figure 3.

Table 2. Instantaneous features used to represent sEMG signal

Temporal Features	Formula	Physical Interpretation	Literature
$< f^0 \mid t >$	$\int C(t,\omega)d\omega$	Intensity: Directly related to muscle voluntary contraction force	[7], [41], [42]
$< f^1 \mid t >$	$\int \frac{C(t,\omega)}{< f^0 \mid t >}\omega d\omega$	Mean frequency: Most widely accepted indicators to NMS system performance	[7], [41], [42]
$< f^2 \mid t >$	$\int \frac{C(t,\omega)}{< f^0 \mid t >}\omega^2 d\omega$	2nd order moment: Related to variance of normalized mean frequency	[43], [44]
$< S \mid t >$	$\int \frac{C(t,\omega)}{< f^0 \mid t >} \ln \frac{C(t,\omega)}{< f^0 \mid t >} d\omega$	Entropy: Describe the non-Gaussianity of instantaneous TFD	[43], [45]

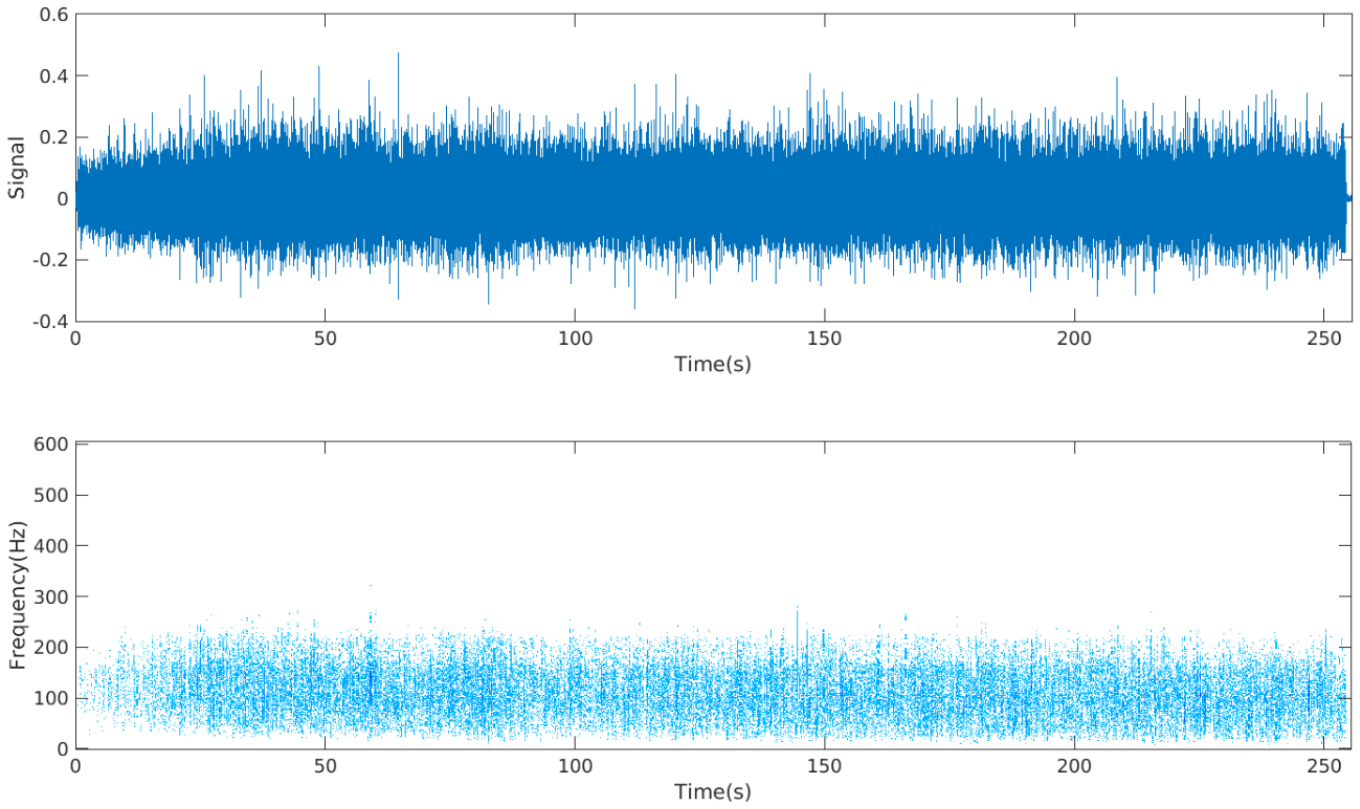

Figure 2. Example of sEMG signals and corresponding TFD

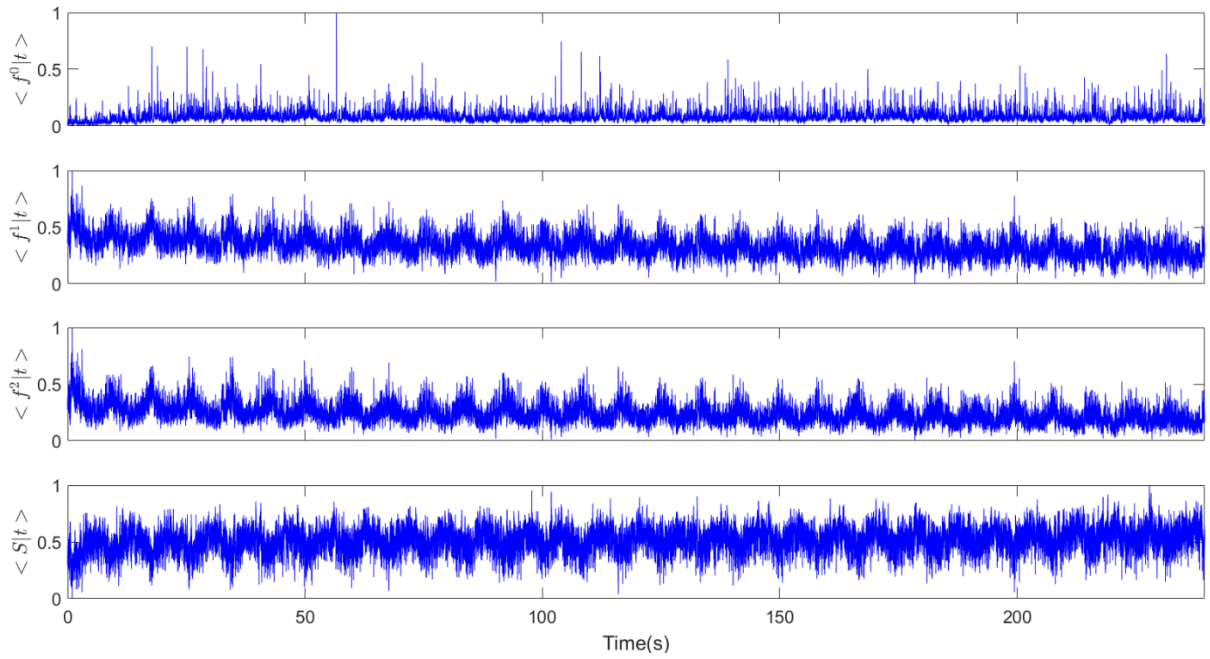

Figure 3. Extracted time series of features from TFD

In order to capture his/her least degraded dynamics, an ARMAX model is built using the data collected at the beginning of his/her exercise or activity. This ARMAX model utilizes time series of temporal features extracted from sEMG signals as system inputs, and the measurements of the relevant limb forces and movements as system outputs. The model learnt in the least degraded (least fatigued) state will be referred to as "fresh model" and the corresponding data will be termed "fresh data". After obtaining the fresh model, a distribution of 1 step ahead prediction errors produced by the model, denoted by *P*, can be generated using the fresh data. This distribution describes how well the inferred fresh model approximates the least degraded NMS system dynamics and will be used as a reference distribution of modeling errors in model-based monitoring.

As newly collected data becomes available, a distribution of most recent 1-step ahead prediction errors is generated using the fresh model. Let this distribution be denoted by Q_T, where T denotes the time interval over which the NMS system performance is evaluated. If the NMS system dynamics remains unchanged, the distributions P and Q_T are expected to be similar to each

other. However, when there is degradation in the NMS system, e.g. due to fatigue or injury, the distribution Q_T will deviate from the fresh distribution P and this deviation can be used to quantitatively differentiate the degradation process. Similarity between distribution P and Q_T will be evaluated via the Kullback Leibler (KL) Divergence measure.

$$FSI = D_{KL}(P \,||\, Q_T) = \sum_{i=1}^{N} P(i) \ln \frac{P(i)}{Q_T(i)} \tag{2}$$

and referred to as the freshness similarity index (FSI). It can be viewed as a quantitative measure describing the discrepancy between the original and degraded system dynamics. Additionally, the model-based monitoring method enables more granular performance characterization at muscle level. When at a new time interval *T*, new sEMG features u_T and physiological measurements y_T are observed. The ARMAX model between muscle signatures and the corresponding limb movement/force variables can be updated to track changes in the NMS system dynamics. In this thesis, the newly learned model, referred to as "updated model", is estimated using steepest gradient descent, initialized from the parameters of the fresh model [46].

Based on the updated model, the performance of an individual muscle *i* over time interval *T* can be assessed by the similarity of dynamic responses from sEMG inputs[1] to system output between the fresh model and the updated model. Following [7], corresponding frequency responses obtained from fresh and updated models will be used for this purpose. Let $H_{T_0}^{i,k}(j\omega)$ denote the frequency response of the fresh model between the k^{th} instantaneous feature of muscle *i* to the system output (limb force or velocity), where $\omega \in [0, \omega_N]$, ω_N is the Nyquist frequency, $k \in \{1,2,3,4\}$, since we extract 4 instantaneous features from each muscle's sEMG signals. Similarly, let $H_T^{i,k}(j\omega)$ denote the frequency response of the updated model between the k^{th} instantaneous feature of muscle *i* to the system output. Following [7], a measure of similarity between these two

[1] instantaneous features relevant to the muscle *i*

frequency responses relating k^{th} feature of muscle i and the system output over time interval T can be expressed as

$$D_T^{i,k} = \frac{\int_0^{\omega_N} \left[\min\left(\left| \mathrm{H}_{T_0}^{i,k}(\mathrm{j}\omega) \right|, \left| \mathrm{H}_T^{i,k}(\mathrm{j}\omega) \right| \right) - \mathrm{c} \right] d\omega}{\int_0^{\omega_N} \left[\max\left(\left| \mathrm{H}_{T_0}^{i,k}(\mathrm{j}\omega) \right|, \left| \mathrm{H}_T^{i,k}(\mathrm{j}\omega) \right| \right) - \mathrm{c} \right] d\omega} \tag{3}$$

where:

- c is the smallest value of $H_T^{i,k}(j\omega)$ and $H_{T_0}^{i,k}(j\omega)$ evaluated in the interval $[0,\omega_{\mathrm{N}}]$;

This measure $D_T^{i,k}$ reflects changes in the model parameters relevant to the k^{th} feature of muscle i, which can be seen as the overlap between $H_{T_0}^{i,k}(j\omega)$ and $H_T^{i,k}(j\omega)$. Nevertheless, in order to analyze performance degradation of muscle i, all the relevant $D_T^{i,k}$ should be combined to evaluate changes in all the model parameters that are relevant to muscle i. In this thesis, a newly defined measure of similarity, characterizing the performance of muscle i over time interval T, is referred to as "muscle-level freshness similarity index" (MFSI) and defined as

$$MFSI_T^i = \frac{\left\| \left(D_T^{i,1}, D_T^{i,2}, D_T^{i,3}, D_T^{i,4} \right) \right\|_2}{2} \tag{4}$$

where:

- $MFSI_T^i$ is the MFSI of muscle i evaluated over time interval T

This measure (MFSI) ranges from 0 to 1, with 1 suggesting perfect match between dynamic interactions relating the sEMG inputs from muscle i to system output for the fresh model and that corresponding to the updated model.

Chapter 4.
Experiment Result and Discussion

In this section, we evaluate the effectiveness of the proposed model-based approach to NMS system performance monitoring using 2 data sets[2]: one collected from an activity related to lower part of the leg and the other collected from a temporomandibular joint (TMJ) system.

4.1. Lower Limb Muscle Constant Contraction Data Set

4.1.1. Experiment Setup and Experimental Protocol

In this data set, sEMG signals were collected from a calf muscle Soleus (SO). Illustrated in Figure 4, SO is an important and strong muscle in the leg, which was active in the isometric plantar flexion the subject performed [47]. As sEMG signals from SO are accessible and the output plantar flexion force is measurable, the experiment provided us an opportunity to study NMS system dynamics changes during exercise and recovery.

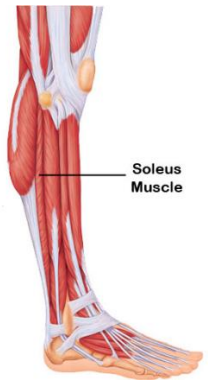

Figure 4. Leg muscle Soleus

[2] These data sets were recorded to validate the proposed algorithms and not used for human subjects' research. Relevant documents are provided as supplemental files.

One male subject with no neuromuscular diseases participated the experiment. During the signal collection process, the subject was seated in a chair with the right thigh fixed. At the same time, the subject's lower leg was fully supported on a pedal, with the right knee flexed at 90 degree, as shown in Figure 5. The plantar flexion force was recorded using S beam load cell (ANYLOAD Company [48]), while the sEMG signals from SO were collected simultaneously through pre-gelled silver/silver chloride disposable electrodes, with the subject's knee serving as reference. The data acquisition was facilitated by Lab Linc V system (Coulbourn Instruments [49]), at the sampling rate of 1212Hz. Frequencies below 8Hz were filtered out by an inbuilt high pass filter to remove influence from the human body and the environment. Multiple notch filters implemented in MATLAB were used to filter out the power line noise (60Hz) and its harmonics.

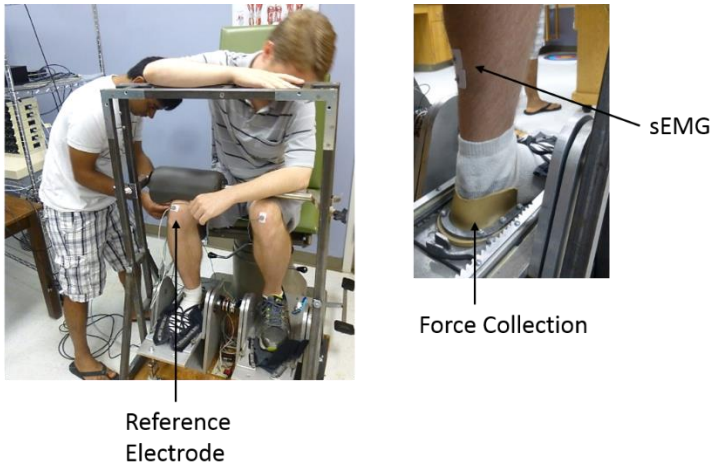

Figure 5. Experiment setup for plantar flexion data set

Before the experiment, the maximum voluntary contraction (MVC) force of the subject was firstly estimated as a reference level. During the experiment, the subject tried to maintain 75% of his maximum voluntary contraction (MVC) by observing output force on the computer screen. The subject would end the exercise when he could not maintain the force above 60% of his MVC

force. After that, the subject repeatedly rested for a minute, followed by a brief 6 ~ 8 second long constant plantar flexion contraction. This cycle of rest-brief plantar flexion contractions was repeated 6 times and the relevant sEMG and force data were collected throughout. Figure 6 illustrates how the plantar flexion contraction force changed with respect to time, with force being normalized by the maximum contraction force in the process.

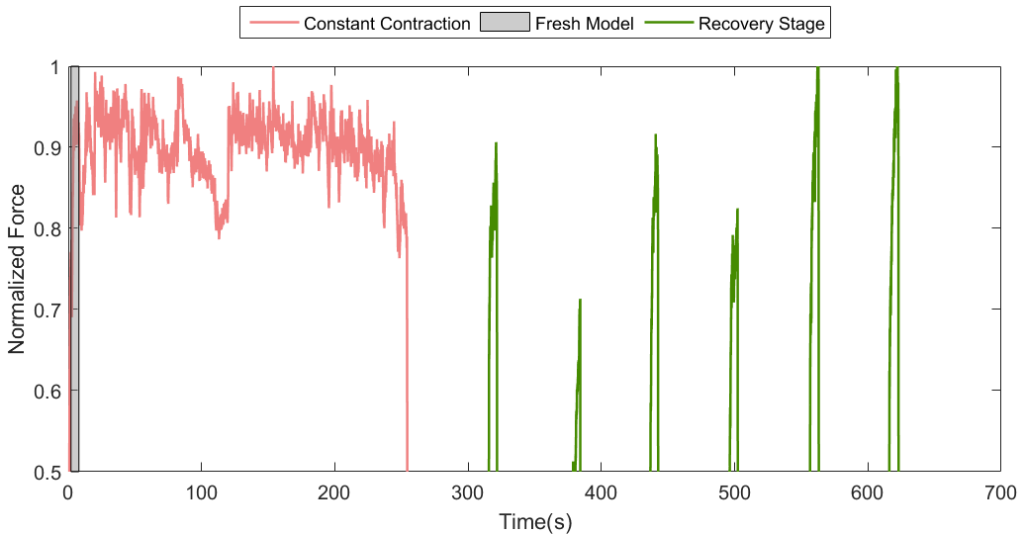

Figure 6. Normalized contraction force over time

4.1.2. Feature Extraction

Figure 7 depicts the sEMG features $< f^0|t >$, $< f^1|t >$, $< f^2|t >$ and $< S|t >$ for the subject in the study. We can observed a statistically significant decreasing trend [3] in the instantaneous mean frequencies $< f^1|t >$ of the SO sEMG signals, which is not a surprise, since it is a classic indicator of muscular fatigue [20]. Furthermore, statistically significant increasing trend in instantaneous intensities $< f^0|t >$ is yet another, perhaps less widely accepted indicator of muscular fatigue [51].

[3] Statistical significance was assessed via a one-sided T test, at the 95% confidence interval [50].

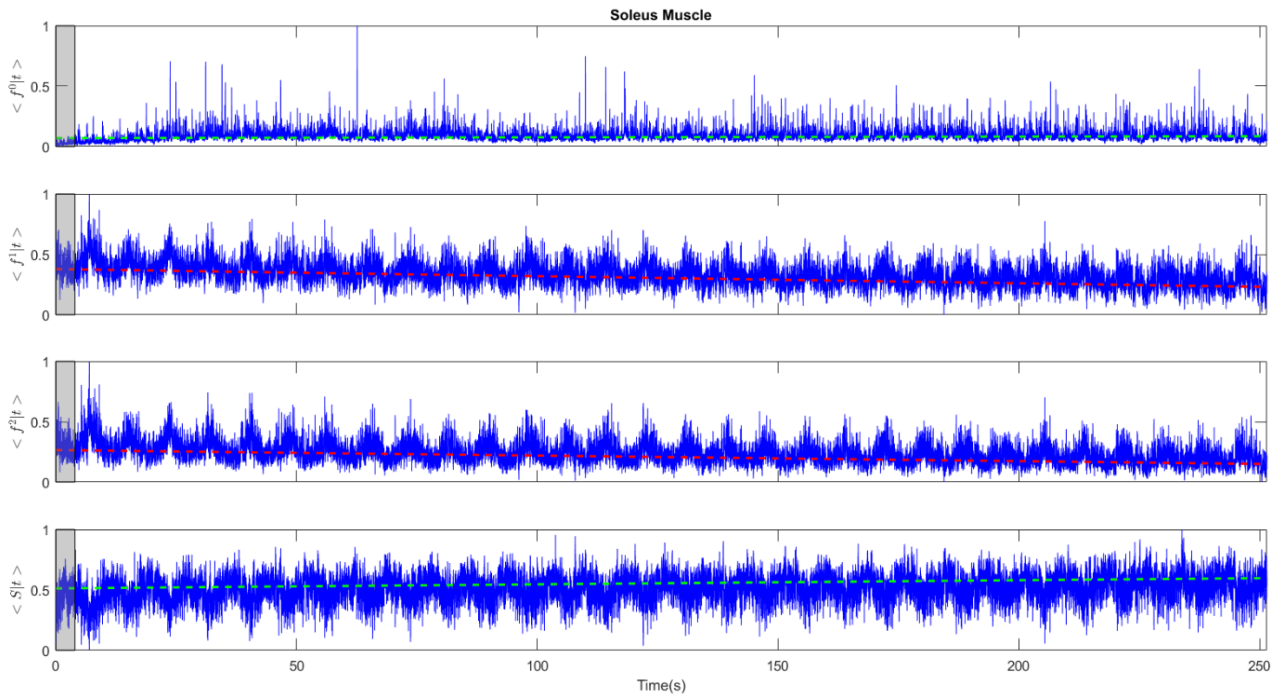

Figure 7. sEMG signatures for data set 1. From top to bottom, the rows of plots in this figure represent features $< f^0|t >$, $< f^1|t >$, $< f^2|t >$ and $< S|t >$ respectively. In all the rows, statistically significant negative trends are indicated with a red dash line while statistically significant positive trends are indicated with a green dash line. The area shaded in gray represents the fresh data. All the features are normalized to the range [0,1]

4.1.3. Monitoring Results

The initial 4s of data in the 75% MVC period was used to train the fresh model. The rest of data were cut into multiple non-overlapping segments, with each segment containing 4s of data. Following [52], the relevant NMS system is modeled as a 2nd order dynamic system, yielding 2nd order ARMAX models. As a result, the fresh model had AR order of 2, input order of 1 and MA order of 1. The FSI was evaluated in each segment to quantify NMS system performance. For the recovery period, we evaluated FSI for each brief plantar flexion contractions period, which gave NMS system performance over that period.

Figure 8 illustrates how FSI changed with respect to time. A statistically significant increase in FSI ($p<0.05$) was observed during the constant contraction stage, while a statistically significant decline in FSI ($p<0.05$) was also observed in the recovery stage. This behavior supported the intuition that, the subject gradually fatigued while maintaining the constant force level, while the subject's NMS system slowly regained normal performance during the recovery stage. The bottom part of Figure 8 depicts the movements of the underlying modeling error distributions generated by the fresh model in the relevant data sections. During the constant contraction period, a shift of the distributions of 1 step ahead prediction errors was clearly visible. Conversely, during the recovery stage, the distribution of 1 step ahead prediction errors gradually returned to again match to a large degree the fresh error distribution. The aforementioned observations match the intuition of expected NMS system changes during exercise and recovery stages.

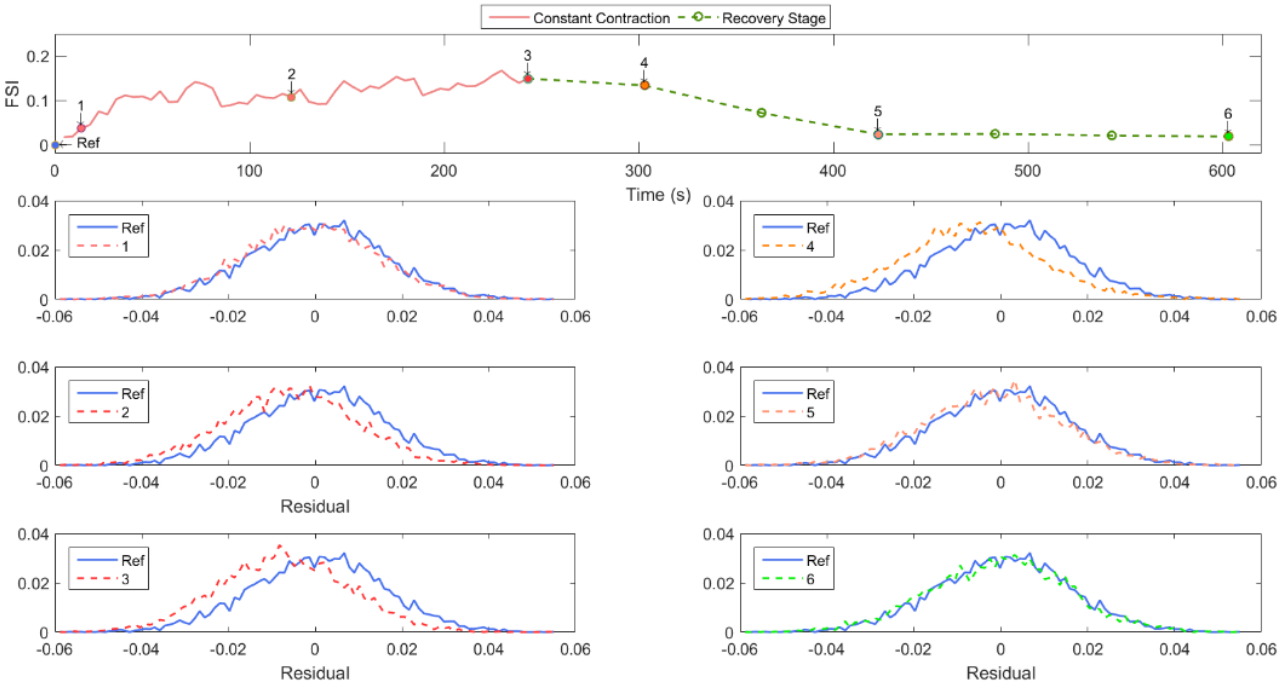

Figure 8. FSI during constant contraction and recovery process

Continuing with the results given above, the MFSI during constant plantar flexion contraction period shows a statistically negative trend ($p<0.05$) as can be seen in Figure 9. This indicates gradual increasing degradation in the performance of incorporated muscle (SO) over time.

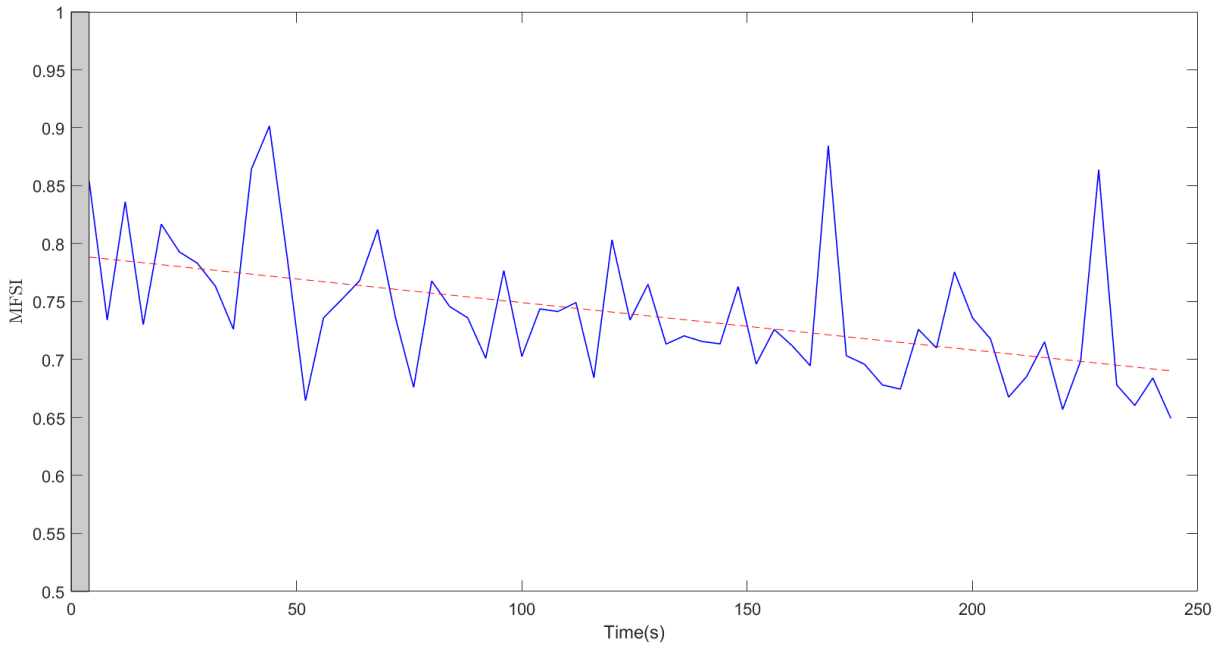

Figure 9. MFSI during constant plantar flexion. Gray patches represent fresh data.

4.2. Temporomandibular Joint (TMJ) Cyclic Motion Data Set

4.2.1. Experiment Setup and Experimental Protocol

sEMG signals from the following six facial muscles were collected from one subject: right temporalis (TA-R), left temporalis (TA-L), right depressor (DA-R), left depressor (DA-L), right masseter (MM-R) and left masseter (MM-L). Figure 10 shows locations of the muscles.

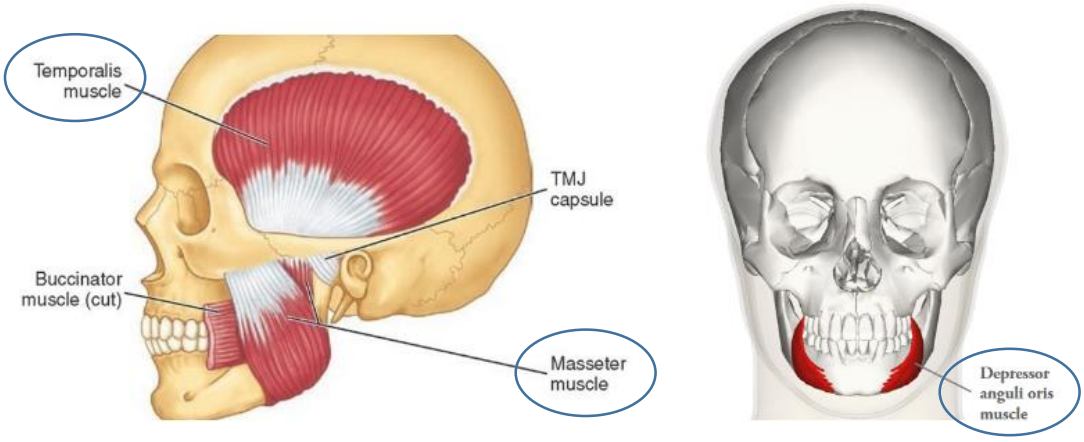

Figure 10. Muscles incorporated in the experiment

One male subject with no neuromuscular diseases participated in the experiment. During the signal collection process, the subject was seated in a chair with a magnet-based 3 dimensional jaw tracker (BioResearch Associates, Inc. [53]) installed to the subject's head for recording jaw motions, as shown in Figure 11. Concurrently, sEMG signals were collected through BioFlex EMG electrodes (BioResearch Associates, Inc. [53]). Both the sEMG signals and jaw velocity were collected at the sampling rate of 2000 Hz. In the experiment, the subject continuously opened and closed mouth without any constraint for 2 minutes. After taking sufficient rest for muscle pain to go away, the subject conducted the experiment again for around half a minute. A set of off-line notch filters, implemented in BioPAK (BioResearch Associates, Inc. [53]), was used to filter out power line noise (60 Hz) and its harmonics.

Figure 11. Experiment setup for TMJ cyclic motion data set. The left figure shows the subject involved in the experiment, while the right figure presents the magnet-based 3D jaw tracker

4.2.2. Feature Extraction

Figure 12 shows the collected sEMG signals for different muscles and their corresponding TFDs. The corresponding jaw velocity is presented in the bottom plot of left column in this figure.

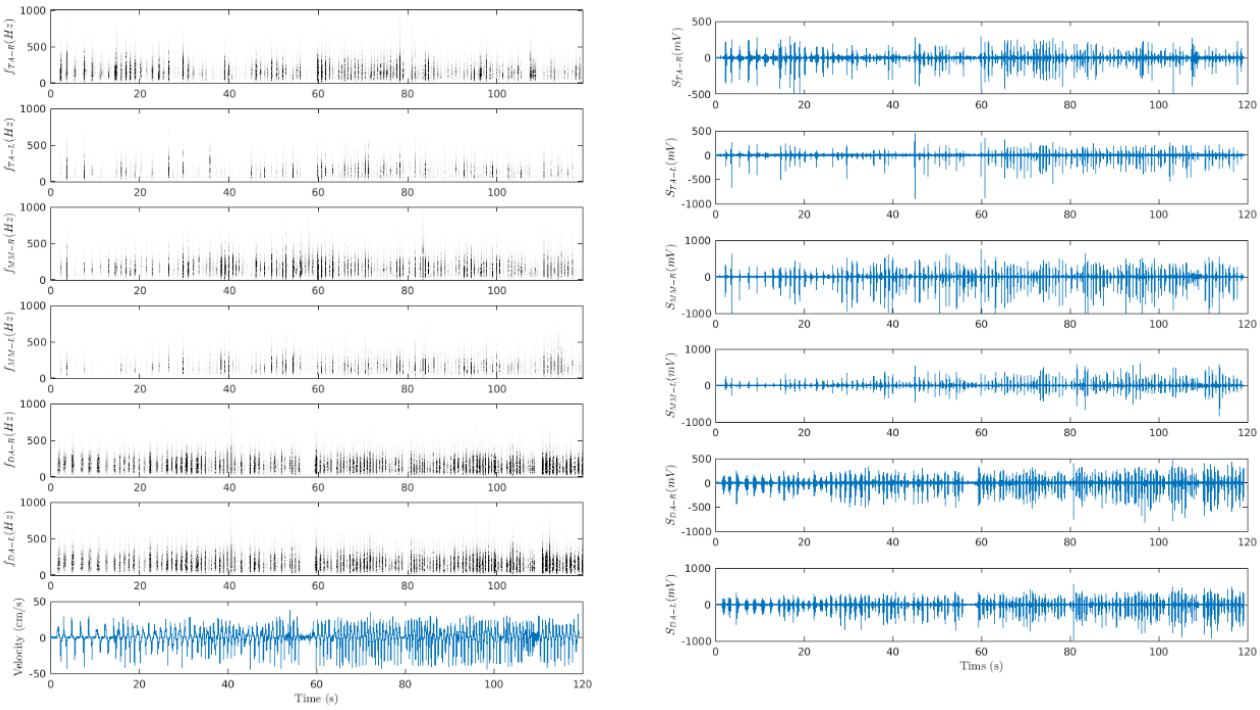

Figure 12. Signals and their TFDs for data set 2.The upper 6 plots in the left column of this figure shows TFD of all incorporated muscles while the bottom plot of left column presents jaw velocity during the motion. The right column of plots shows original sEMG signals collected from different muscles.

Figure 13 depicts the sEMG features $< f^0|t >$ and $< f^1|t >$ for the subject in the study. It can be seen that 5 out of 6 muscles had shown statistically significant positive trend ($p<0.05$) in $< f^0|t >$, while all of the muscles show statistically significant negative trend ($p<0.05$) in $< f^1|t >$. This is consistent with $< f^1|t >$ and $< f^0|t >$ being classic indicators of muscle fatigue [20].

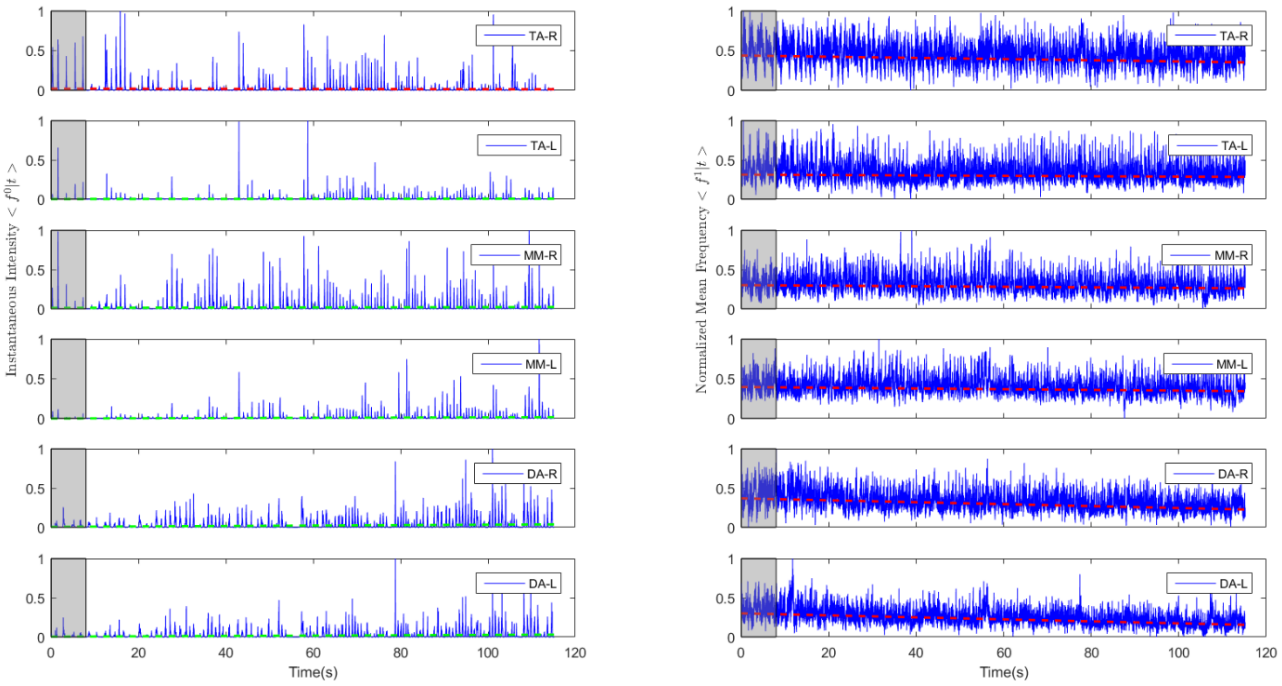

Figure 13. sEMG signatures $< f^0|t >$ and $< f^1|t >$ for data set 2.The left column of plots in this figure shows $< f^0|t >$ features, while the right column of plots shows $< f^1|t >$ features. In both columns, statistically significant negative trends are indicated with a red dash line while statistically significant positive trends are indicated with a green dash line. The area shaded in gray represents the fresh data. All the features are normalized to the range [0,1]

Figure 14 depicts the sEMG features $< f^2|t >$ and $< S|t >$ for the subject in the study. It was noticed that $< f^2|t >$ in all the muscles had shown statistically significant negative trends ($p<0.05$), while $< S|t >$ had shown statistically significant positive trends ($p<0.05$) in TA-R DA-R, DA-L MM-L, and statically significant negative trends ($p<0.05$) in TA-L and MM-R. Current literature does not seem to be able to establish a consistent link between trends in $< f^2|t >$ and $< S|t >$ to muscle fatigue.

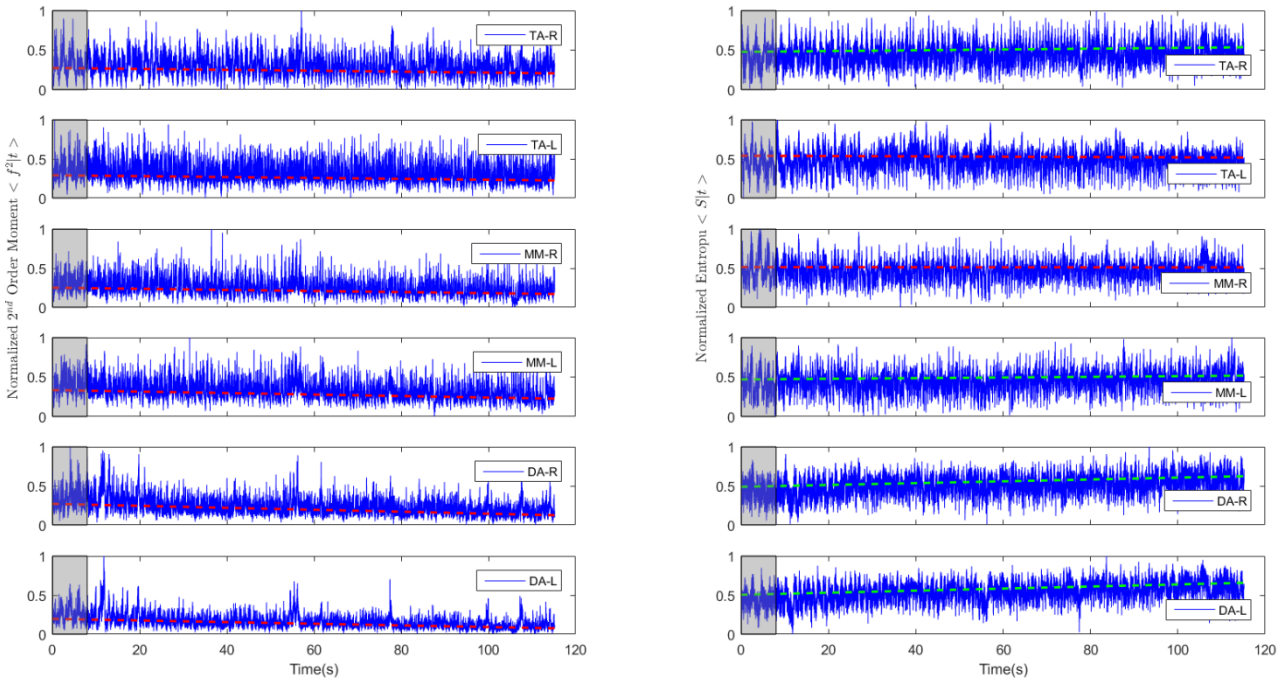

Figure 14. sEMG signatures $< f^2|t >$ and $< S|t >$ for data set 2. The left column of plots in this figure shows $< f^2|t >$ features, while the right column of plots shows $< S|t >$ features. In both columns, statistically significant negative trends are indicated with a red dash line while statistically significant positive trends are indicated with a green dash line. The area shaded in gray represents the fresh data. All the features are normalized to the range [0,1]

4.2.3. Monitoring Results

The first 8s of the data was used to train the fresh model. The rest of data were cut into multiple non-overlapping segments in 6 second time horizon, with FSI evaluated in each segment of data. We modeled each pair of muscles as a 2nd order system (mass spring dashpot system), yielding a 6th order ARMAX model. Therefore, the fresh model had AR order of 6, input order of 5 and MA order of 5.

Figure 15 illustrates how FSI changed with respect to time. A statistically significant increase in FSI ($p<0.05$) was observed when the subject was performing the 1st cyclic motion. It is also evident that after taking sufficient rest, FSI went back to its original level. This behavior again supports the intuition that during continuous cyclic motion, the subject gradually got fatigued, while the subject's NMS system regained normal performance after rest. The bottom part of Figure 15 depicts the changes in modeling error distribution. In the 1st round of cyclic jaw opening and closing, a gradual changes in the error distribution of 1 step ahead model predictions is obviously observed (points labeled 1, 2 and 3). After rest, the error distribution of 1 step ahead predictions returned back to again match with the fresh error distribution (the point labeled 4). The aforementioned observations also match the intuition of NMS system changes during continuous cyclic motions and recovery processes.

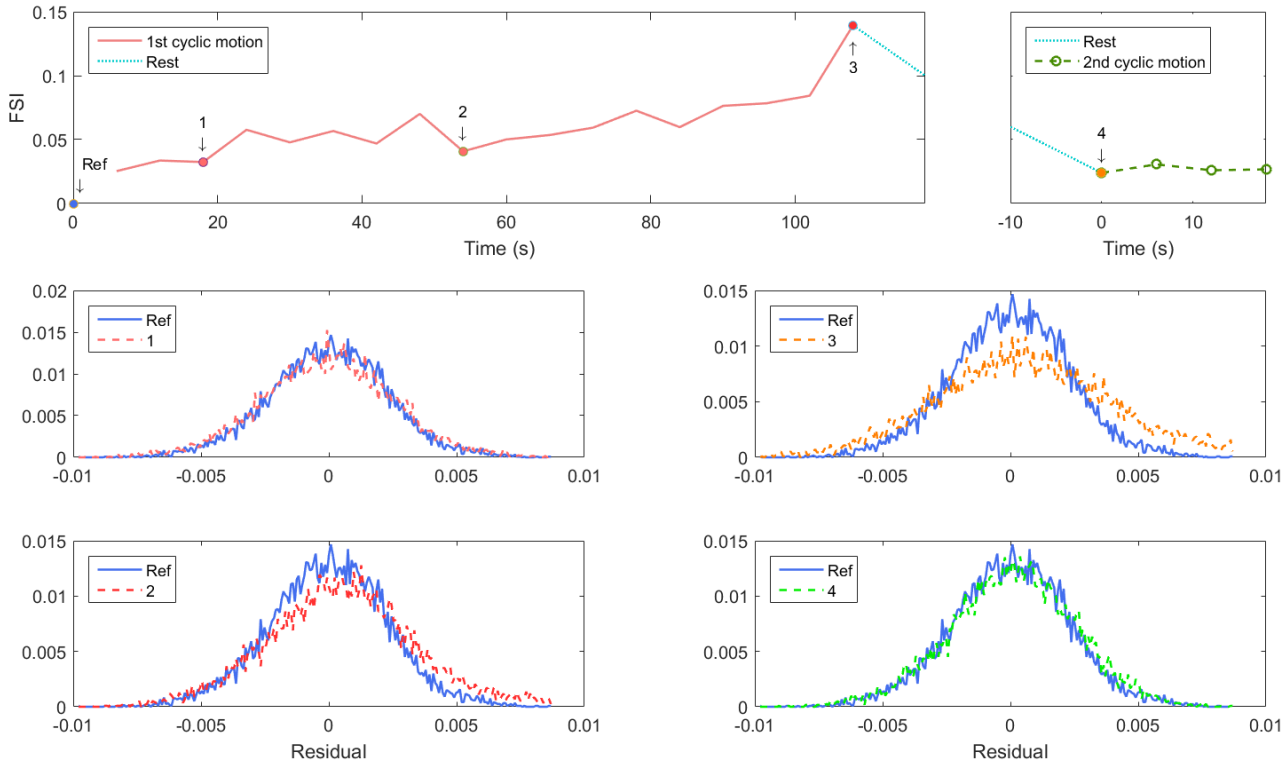

Figure 15. FSI for the 1st and 2nd cyclic motion

In this data set, there were 6 muscles (3 pairs of muscles) associated the motion. The relevant muscle-level performance indices MFSI are shown in Figure 16. Statistically significant negative trends ($p<0.05$) in MFSI were observed among all the muscles, illustrating performance degradation of corresponding muscles. Specifically, it was noticed that MM-R and MM-L had more significant decreasing trend ($p<0.001$) in MFSI compared to other muscles, as evident from Table 3. This behavior is consistent with the fact that MM-R and MM-L contributed the most (work the most) in the performed cyclic motion.

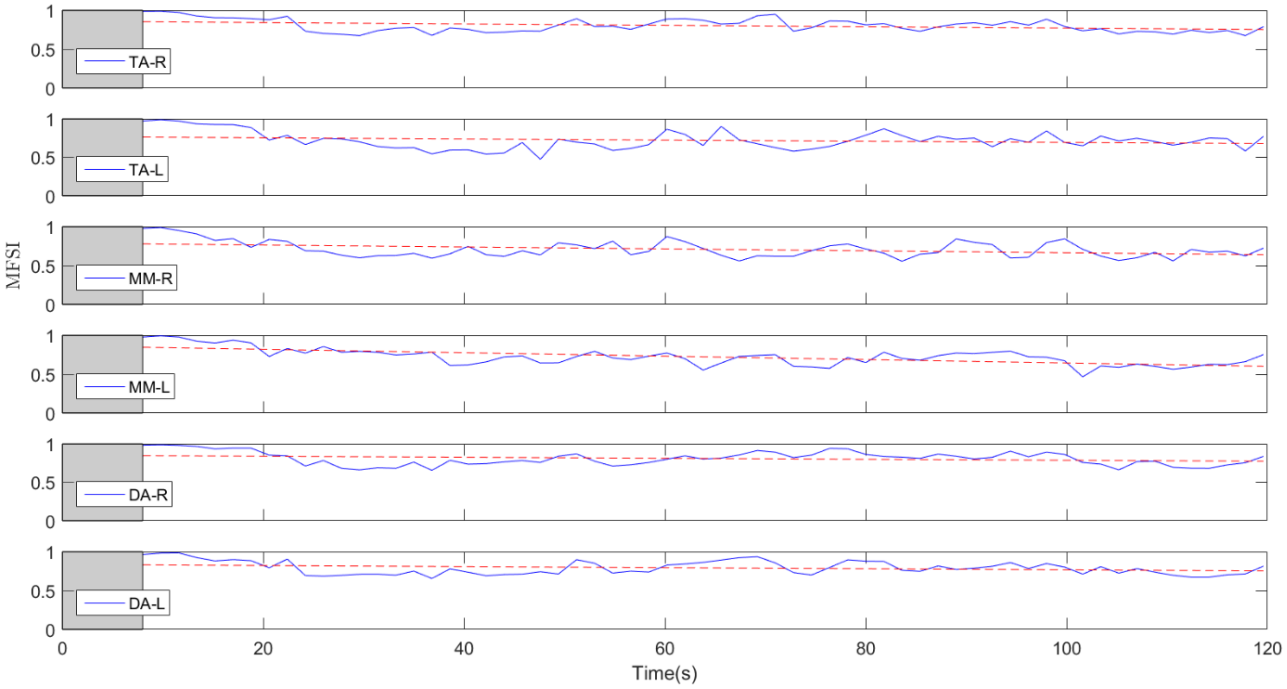

Figure 16. MFSI for the 1st cyclic motion. Gray patches represent fresh data.

Table 3. Slopes of MFSI over time in the 1st cyclic motion

Muscle	TA-R	TA-L	MM-R	MM-L	DA-R	DA-L
Slope	-8.9825e-04	-7.5230e-04	-0.0012	-0.0022	-6.4292e-04	-6.8751e-04

Chapter 5.
Conclusion & Future Work

5.1. Conclusions

Research presented in this thesis focused on developing model based approaches for monitoring performance degradation and recovery of different portions of NMS system. Furthermore, the proposed method enabled characterization of NMS system performance degradation at muscle level. Monitoring of NMS system performance was realized via statistical analysis of modeling error generated by the ARMAX model relating instantaneous intensities, expected frequencies, 2nd order moments and entropies extracted from each muscle's sEMG signals with physiological outputs. At the muscle level, performance degradation of a specific muscle in the NMS system was characterized by tracking changes in the transfer functions related to that muscle.

This thesis discussed the findings coming from two different data sets, one collected from an activity related to lower limb muscles and the other collected from TMJ muscles. In both data sets, the model-based approach successfully detected statistically significant trends representing NMS system performance degradation as exercise progressed. Furthermore, recoveries to original system performance were observed after subjects had sufficient rest. In addition, the model-based muscle-level performance characterization successfully demonstrated degradation in all the relevant muscles and identified those muscles that degraded the most in the designated motions.

5.2. Future Work

Advancements in the model-based monitoring of NMS system could facilitate personalizing and customizing of training regimens for athletes and patients undergoing rehabilitation by prescribing exercises. E.g., for athletes, detection and characterization of NMS system performance

degradation and recovery can be used as an indication to stop training before the onset of injury, and start training again when muscles recover. Potential future works can further concentrate on the following three aspects. Firstly, the dynamic model used in this thesis assume linear relationships between system inputs and outputs, which is analytically tractable but not appropriate for NMS system modeling. Therefore, developing nonlinear dynamic models could better approximate NMS system dynamics and enable more accurate performance monitoring. Furthermore, as muscles coordinate with each other during movement [54], modeling coordination between different muscles in the dynamic models could further enhance the muscle-level performance characterization, such as linking instantaneous features between different muscles. Finally, as the number of participants, incorporated motions and portions of NMS system were limited in our two data sets, the model-based monitoring techniques should be further explored on larger data sets corresponding to different portions of NMS system and rapidly changing motions, such as monitoring leg muscles during cycling.

Bibliography

[1] A. K. Jardine, D. Lin, and D. Banjevic, "A review on machinery diagnostics and prognostics implementing condition-based maintenance," *Mech. Syst. Signal Process.*, vol. 20, no. 7, pp. 1483–1510, 2006.

[2] R. Kothamasu, S. H. Huang, and W. H. VerDuin, "System health monitoring and prognostics–a review of current paradigms and practices," in *Handbook of Maintenance Management and Engineering*, Springer, 2009, pp. 337–362.

[3] R. Isermann, "Model-based fault-detection and diagnosis–status and applications," *Annu. Rev. Control*, vol. 29, no. 1, pp. 71–85, 2005.

[4] J. B. Dingwell, D. F. Napolitano, and D. Chelidze, "A nonlinear approach to tracking slow-time-scale changes in movement kinematics," *J. Biomech.*, vol. 40, no. 7, pp. 1629–1634, 2007.

[5] D. B. Segala, D. H. Gates, J. B. Dingwell, and D. Chelidze, "Nonlinear Smooth Orthogonal Decomposition of Kinematic features of sawing reconstructs muscle fatigue evolution as indicated by electromyography," *J. Biomech. Eng.*, vol. 133, no. 3, p. 031009, 2011.

[6] N. K. Vøllestad, "Measurement of human muscle fatigue," *J. Neurosci. Methods*, vol. 74, no. 2, pp. 219–227, 1997.

[7] M. W. Musselman, "Monitoring of biomedical systems using non-stationary signal analysis," 2013.

[8] A. R. Kralj and T. Bajd, *Functional electrical stimulation: standing and walking after spinal cord injury*. CRC press, 1989.

[9] R. R. Bini, F. Diefenthaeler, and C. B. Mota, "Fatigue effects on the coordinative pattern during cycling: Kinetics and kinematics evaluation," *J. Electromyogr. Kinesiol.*, vol. 20, no. 1, pp. 102–107, 2010.

[10] J. D. Chappell, D. C. Herman, B. S. Knight, D. T. Kirkendall, W. E. Garrett, and B. Yu, "Effect of fatigue on knee kinetics and kinematics in stop-jump tasks," *Am. J. Sports Med.*, vol. 33, no. 7, pp. 1022–1029, 2005.

[11] K. A. Christina, S. C. White, and L. A. Gilchrist, "Effect of localized muscle fatigue on vertical ground reaction forces and ankle joint motion during running," *Hum. Mov. Sci.*, vol. 20, no. 3, pp. 257–276, 2001.

[12] D. H. Gates and J. B. Dingwell, "The effects of neuromuscular fatigue on task performance during repetitive goal-directed movements," *Exp. Brain Res.*, vol. 187, no. 4, pp. 573–585, 2008.

[13] M. Reaz, M. Hussain, and F. Mohd-Yasin, "Techniques of EMG signal analysis: detection, processing, classification and applications," *Biol. Proced. Online*, vol. 8, no. 1, pp. 11–35, 2006.

[14] R. Merletti and P. A. Parker, *Electromyography: physiology, engineering, and non-invasive applications*, vol. 11. John Wiley & Sons, 2004.

[15] S. Shahid, J. Walker, G. M. Lyons, C. Byrne, A. V. Nene, and others, "Application of higher order statistics techniques to EMG signals to characterize the motor unit action potential," *Biomed. Eng. IEEE Trans. On*, vol. 52, no. 7, pp. 1195–1209, 2005.

[16] R. D. Keynes, D. J. Aidley, and C. L.-H. Huang, *Nerve and muscle*. Cambridge Univ Press, 2001.

[17] B. Gerdle, B. Larsson, and S. Karlsson, "Criterion validation of surface EMG variables as fatigue indicators using peak torque: a study of repetitive maximum isokinetic knee extensions," *J. Electromyogr. Kinesiol.*, vol. 10, no. 4, pp. 225–232, 2000.

[18] M. M. Morlock, V. Bonin, G. Müller, and E. Schneider, "Trunk muscle fatigue and associated EMG changes during a dynamic iso-inertial test," *Eur. J. Appl. Physiol.*, vol. 76, no. 1, pp. 75–80, 1997.

[19] M. Cifrek, V. Medved, S. Tonković, and S. Ostojić, "Surface EMG based muscle fatigue evaluation in biomechanics," *Clin. Biomech.*, vol. 24, no. 4, pp. 327–340, 2009.

[20] W. Ament, G. J. Bonga, A. L. Hof, and G. J. Verkerke, "EMG median power frequency in an exhausting exercise," *J. Electromyogr. Kinesiol.*, vol. 3, no. 4, pp. 214–220, 1993.

[21] A. Phinyomark, C. Limsakul, H. Hu, P. Phukpattaranont, and S. Thongpanja, *The usefulness of mean and median frequencies in electromyography analysis*. INTECH Open Access Publisher, 2012.

[22] G. V. Dimitrov, T. I. Arabadzhiev, K. N. Mileva, J. L. Bowtell, N. Crichton, and N. A. Dimitrova, "Muscle fatigue during dynamic contractions assessed by new spectral indices," *Med. Sci. Sports Exerc.*, vol. 38, no. 11, p. 1971, 2006.

[23] R. Merletti, A. Gulisashvili, and L. R. Lo Conte, "Estimation of shape characteristics of surface muscle signal spectra from time domain data," *Biomed. Eng. IEEE Trans. On*, vol. 42, no. 8, pp. 769–776, 1995.

[24] O. Paiss and G. F. Inbar, "Autoregressive modeling of surface EMG and its spectrum with application to fatigue," *Biomed. Eng. IEEE Trans. On*, no. 10, pp. 761–770, 1987.

[25] M. Cifrek, S. Tonković, and V. Medved, "Measurement and analysis of surface myoelectric signals during fatigued cyclic dynamic contractions," *Measurement*, vol. 27, no. 2, pp. 85–92, 2000.

[26] S. H. Roy, P. Bonato, and M. Knaflitz, "EMG assessment of back muscle function during cyclical lifting," *J. Electromyogr. Kinesiol.*, vol. 8, no. 4, pp. 233–245, 1998.

[27] P. Bonato, S. H. Roy, M. Knaflitz, and C. J. De Luca, "Time-frequency parameters of the surface myoelectric signal for assessing muscle fatigue during cyclic dynamic contractions," *Biomed. Eng. IEEE Trans. On*, vol. 48, no. 7, pp. 745–753, 2001.

[28] D. K. Kumar, N. D. Pah, and A. Bradley, "Wavelet analysis of surface electromyography," *Neural Syst. Rehabil. Eng. IEEE Trans. On*, vol. 11, no. 4, pp. 400–406, 2003.

[29] D. Korošec, “Continuous time-varying autoregressive spectrum for assessment of fatigue induced changes in SEMG signals,” in *[Engineering in Medicine and Biology, 1999. 21st Annual Conference and the 1999 Annual Fall Meetring of the Biomedical Engineering Society] BMES/EMBS Conference, 1999. Proceedings of the First Joint*, 1999, vol. 1, p. 574–vol.

[30] Wikipedia, *Hill’s muscle model — Wikipedia, The Free Encyclopedia*. 2014.

[31] K. Manal and T. S. Buchanan, “A one-parameter neural activation to muscle activation model: estimating isometric joint moments from electromyograms,” *J. Biomech.*, vol. 36, no. 8, pp. 1197–1202, 2003.

[32] F. Moosavi, A. Pasdar, H. Ehsani, and M. Rostami, “An EMG-driven musculoskeletal model to predict muscle forces during performing a weight training exercise with a dumbbell,” in *Biomedical Engineering (ICBME), 2012 19th Iranian Conference of*, 2012, pp. 79–84.

[33] D. G. Lloyd and T. F. Besier, “An EMG-driven musculoskeletal model to estimate muscle forces and knee joint moments in vivo,” *J. Biomech.*, vol. 36, no. 6, pp. 765–776, 2003.

[34] Y. Z. Arslan, M. A. Adli, A. Akan, and M. B. Baslo, “Prediction of externally applied forces to human hands using frequency content of surface EMG signals,” *Comput. Methods Programs Biomed.*, vol. 98, no. 1, pp. 36–44, 2010.

[35] Q. Zhang, M. Hayashibe, P. Fraisse, and D. Guiraud, “FES-induced torque prediction with evoked EMG sensing for muscle fatigue tracking,” *Mechatron. IEEEASME Trans. On*, vol. 16, no. 5, pp. 816–826, 2011.

[36] P. K. Artemiadis and K. J. Kyriakopoulos, “EMG-based teleoperation of a robot arm in planar catching movements using ARMAX model and trajectory monitoring techniques,” in *Robotics and Automation, 2006. ICRA 2006. Proceedings 2006 IEEE International Conference on*, 2006, pp. 3244–3249.

[37] S. Karlsson, J. Yu, and M. Akay, "Time-frequency analysis of myoelectric signals during dynamic contractions: a comparative study," *Biomed. Eng. IEEE Trans. On*, vol. 47, no. 2, pp. 228–238, 2000.

[38] L. Cohen, *Time-frequency analysis*, vol. 1. Prentice hall, 1995.

[39] J. Jeong and W. J. Williams, "Kernel design for reduced interference distributions," *Signal Process. IEEE Trans. On*, vol. 40, no. 2, pp. 402–412, 1992.

[40] A. Papandreou-Suppappola, *Applications in time-frequency signal processing*. CRC press, 2002.

[41] J. Potvin, "Effects of muscle kinematics on surface EMG amplitude and frequency during fatiguing dynamic contractions," *J. Appl. Physiol.*, vol. 82, no. 1, pp. 144–151, 1997.

[42] M. Bilodeau, S. Schindler-Ivens, D. Williams, R. Chandran, and S. Sharma, "EMG frequency content changes with increasing force and during fatigue in the quadriceps femoris muscle of men and women," *J. Electromyogr. Kinesiol.*, vol. 13, no. 1, pp. 83–92, 2003.

[43] M. Musselman and D. Djurdjanovic, "Time–frequency distributions in the classification of epilepsy from EEG signals," *Expert Syst. Appl.*, vol. 39, no. 13, pp. 11413–11422, 2012.

[44] A. Phinyomark, P. Phukpattaranont, and C. Limsakul, "Feature reduction and selection for EMG signal classification," *Expert Syst. Appl.*, vol. 39, no. 8, pp. 7420–7431, 2012.

[45] P. Karthick, G. Venugopal, and S. Ramakrishnan, "Analysis of surface EMG signals under fatigue and non-fatigue conditions using B-distribution based quadratic time frequency distribution," *J. Mech. Med. Biol.*, vol. 15, no. 02, p. 1540028, 2015.

[46] A. Wills and B. Ninness, "On gradient-based search for multivariable system estimates," *Autom. Control IEEE Trans. On*, vol. 53, no. 1, pp. 298–306, 2008.

[47] M. Bilodeau, C. Goulet, S. Nadeau, A. B. Arsenault, and D. Gravel, "Comparison of the EMG power spectrum of the human soleus and gastrocnemius muscles," *Eur. J. Appl. Physiol.*, vol. 68, no. 5, pp. 395–401, 1994.

[48] “ANYLOAD Transducer.” [Online]. Available: http://www.anyload.com/. [Accessed: 25-Apr-2016].

[49] “Coulbourn Instruments.” [Online]. Available: http://www.coulbourn.com/. [Accessed: 25-Apr-2016].

[50] D. C. Montgomery, G. C. Runger, and N. F. Hubele, *Engineering statistics*. John Wiley & Sons, 2009.

[51] G. R. Pereira, L. F. de Oliveira, and J. Nadal, “Isometric fatigue patterns in time and time–frequency domains of triceps surae muscle in different knee positions,” *J. Electromyogr. Kinesiol.*, vol. 21, no. 4, pp. 572–578, 2011.

[52] S. M. Pandit, S.-M. Wu, and others, *Time series and system analysis with applications*. Wiley New York, 1983.

[53] “BioResearch.” [Online]. Available: https://www.bioresearchinc.com/. [Accessed: 26-Apr-2016].

[54] F. E. Zajac, “Muscle coordination of movement: a perspective,” *J. Biomech.*, vol. 26, pp. 109–124, 1993.